Emulsion Polymerization of *N*-Ethylacrylamide in Supercritical Carbon Dioxide

Weijun Ye[†,‡] and Joseph M. DeSimone[*,†,‡,§]

Department of Chemistry, University of North Carolina at Chapel Hill, CB# 3290, Venable Hall, Chapel Hill, North Carolina 27599-3290, NSF Science and Technology Center for Environmentally Responsible Solvents and Processes, Department of Chemistry, University of North Carolina at Chapel Hill, CB# 3290, Venable Hall, Chapel Hill, North Carolina 27599-3290, and Department of Chemical Engineering, North Carolina State University, P.O. Box 7905, Raleigh, North Carolina 27695-7905

Received June 9, 2004; Revised Manuscript Received December 21, 2004

ABSTRACT: Herein, we report the emulsion polymerization of a water-soluble vinylic monomer in supercritical carbon dioxide. The water-soluble/CO_2-insoluble monomer, *N*-ethylacrylamide, was effectively emulsified in CO_2 continuous phase using an amphiphilic diblock copolymer consisting of a D-glucose-containing glycopolymer and a fluorinated block. The resulting high yield (>90%) of water-soluble poly(*N*-ethylacrylamide) was obtained in the form of a stable polymer colloid comprised of submicrometer-sized particles. The particle diameter and the distribution of sizes were shown to be influenced by various reaction parameters. Higher temperature and higher surfactant and initiator concentrations resulted in particles with smaller sizes. Two initiators, 2,2′-azobisisobutyronitrile (AIBN) and a fluorinated azo-derivative, bis-[2-(*F*-octyl)ethyl]-4,4′-azobis-4-cyanopentanoate, were used, and their thermal decomposition behaviors in supercritical CO_2 were investigated. Compared with the AIBN-initiated system, the emulsion polymerizations initiated by the fluorinated azo-initiator showed no polymerized monomer droplets, and the resultant particles were more uniform.

Introduction

Recently, the use of supercritical carbon dioxide ($scCO_2$) as an alternative to traditional aqueous and organic solvents has attracted much attention in the fields of polymer synthesis and processing.[1−3] Carbon dioxide is a readily available, inexpensive, nontoxic, and nonflammable natural product with easily accessible supercritical parameters (its critical temperature and pressure being 31.1 °C and 73.8 bar, respectively). These properties render CO_2 a useful and environmentally benign medium compared with current organic solvents. Our group has reported the first homogeneous polymerization in $scCO_2$ to prepare fluoropolymers.[4] Thereafter, heterogeneous polymerizations in liquid and supercritical CO_2 have been studied intensively.[1−3]

Heterogeneous polymerization processes involve at least two phases during polymerizations.[5] The resulting polymers are insoluble in the reaction continuous phase and may be dispersed by the addition of stabilizing additives (surfactants). Since CO_2 is a poor solvent for most macromolecules[6] while monomers are relatively easy to dissolve in CO_2,[7] much research focuses on CO_2-dispersion[8−14] or -precipitation polymerizations,[15−17] in which the initial state of the polymerization mixture is homogeneous. Unlike dispersion or precipitation polymerization, the initial state of emulsion or suspension polymerization is heterogeneous. Monomers, as well as the produced polymers, are not miscible with the reaction medium. The difference between emulsion and suspension polymerization is that, in emulsion polymerization, a medium-soluble initiator can be dissolved into the continuous phase, while in suspension polymerization, the initiator is only soluble in the monomer but not the polymerization medium. The difficulty of performing emulsion or suspension polymerizations in CO_2 is that most of the common monomers are CO_2-soluble. In addition, proper CO_2-soluble surfactants (emulsifiers) are required to emulsify monomers into the CO_2 phase. So far, there are very few reported emulsion polymerizations in CO_2. As a different approach, emulsion polymerizations in hybrid CO_2/water mixtures have been reported.[18,19] Quadir, et al.[18] investigated the emulsion polymerization of methyl methacrylate in a surfactant-free CO_2/water system, in which polymer particles in submicrometer sizes were formed as a stable latex in the aqueous phase. Beckman, et al.[19] synthesized a water-soluble polymer, polyacrylamide, in CO_2/water mixtures with the aid of an amide-functionalized perfluoropolyether surfactant; a more stable milky-white latex was observed during polymerization compared with the system without stabilizer. Most recently, Hile, et al.[20] reported the emulsion copolymerization of D,L-lactide and glycolide in supercritical CO_2 with the help of a fluorocarbon polymer as the emulsifying agent; improved molecular weights and monomer conversions were found versus the syntheses without surfactant.

Recently, we have reported the successful living anionic polymerization of a well-controlled sugar-containing amphiphilic diblock copolymer, poly(3-*O*-methacryloyl-1,2:5,6-di-*O*-isopropylidene-D-glucofuranose-*b*-poly(1,1-dihydroperfluorooctyl methacrylate)(PMAIpGlc-*b*-PFOMA).[21] Removal of acetal protective groups from the protected sugar block yielded a hydrophilic, CO_2-soluble block copolymer, poly(3-*O*-methacryloyl-D-glucopyronose)-*b*-PFOMA (PMAGlc-*b*-PFOMA). With the aid of such a hydrophilic/CO_2-philic diblock copolymer surfactant, we report herein the emulsion polymeriza-

* Author to whom correspondence should be addressed. E-mail: desimone@unc.edu. Tel: 919-962-2164. Fax: 919-962-5467.
† Department of Chemistry, University of North Carolina at Chapel Hill.
‡ NSF Science and Technology Center for Environmentally Responsible Solvents and Processes.
§ Department of Chemical Engineering, University of North Carolina at Chapel Hill.

10.1021/ma048863q CCC: $30.25
Published on Web 02/09/2005

Scheme 1. Diblock Copolymer Synthesis

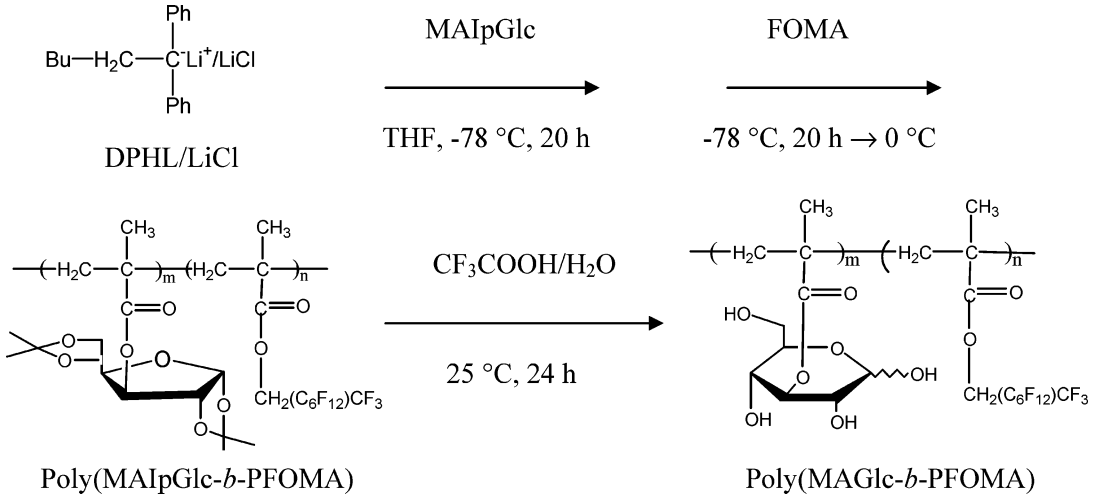

tion of a water-soluble vinylic monomer, *N*-ethylacrylamide (NEAM), in a CO_2 continuous phase to obtain submicrometer-sized polymer particles.

Experimental Section

Materials. 2,2′-Azobisisobutyronitrile (AIBN; Aldrich, Milwaukee, WI) was recrystallized twice from methanol. 1,1-Dihydroperfluorooctyl methacrylate (FOMA; 3 M, St. Paul, MN) was purified by being passed through an alumina column to remove inhibitor and being dried and distilled over CaH_2 twice. 1,1-Diphenylethylene (DPE, Aldrich) was first dried and distilled over CaH_2 and finally distilled from a 1,1-diphenylhexyllithium (DPHL) solution under reduced pressure. Tetrahydrofuran (THF) was refluxed over sodium-benzophenone complex until a persistent deep-purple color was observed. Commercially available *N*-butyllithium (*n*-BuLi, a 1.6 M solution in hexane, Aldrich) was used without further purification. Lithium chloride (LiCl, Aldrich) was dried overnight at 130 °C and dissolved in dry THF. 4,4′-Azobis-4-cyanopentanoic acid (Aldrich) was dried in a vacuum. 1,2:5,6-Di-*O*-isopropylidene-D-glucofuranose, methacrylic anhydride, trifluoroacetic acid, ethylamine (2.0 M in solution in tetrahydrofuran), acryloyl chloride, phosphorus pentachloride, 1,1,2-trichlorotrifluoroethane (Freon-113), anhydrous benzene, ether, hexane, methylene chloride, sodium bicarbonate, and sodium sulfate were all from Aldrich and were used as received. 1,1,2,2-Tetrahydroperfluorodecanol was from Lancaster and used as received. Carbon dioxide (SFE/SFC grade) was provided by Air Products (Allentown, PA) and was used as received.

Synthesis of *N*-Ethylacrylamide. The NEAM monomer was synthesized by the reaction of ethylamine with acryloyl chloride[22] and was further purified under vacuum distillation.

Synthesis of 3-*O*-Methacryloyl-1,2:5,6-di-*O*-isopropylidene-D-glucofuranose (MAIpGlc). The sugar-containing monomer was prepared by the reaction of 1,2:5,6-di-O-isopropylidene-D-glucofuranose with methacrylic anhydride[23−25] and was purified twice by drying over CaH_2 and vacuum distillation.

Diblock Copolymer Synthesis. PMAIpGlc-*b*-PFOMA diblock copolymers were synthesized as previously reported[21] by sequential living anionic polymerization in THF at −78 °C with DPHL in the presence of lithium chloride, and PMAGlc-*b*-PFOMA was obtained after hydrolysis of the sugar blocks (Scheme 1).

Synthesis of Fluorinated Azo-Derivative Initiator. 4,4′-Azobis-4-cyanopentanoyl chloride synthesis followed the method reported by Smith[26] from the reaction of 4,4′-azobis-4-cyanopentanoic acid with phosphorus pentachloride in benzene. The fluorinated initiator, bis-[2-(*F*-octyl)ethyl]-4,4′-azobis-4-cyanopentanoate (Figure 1) was prepared by treating the resultant 4,4′-azobis-4-cyanopentanoyl chloride with a perfluorinated alcohol, 1,1,2,2-tetrahydroperfluorodecanol, in a mixture of THF and Freon-113 under a catalytic amount of pyridine at room temperature.[27] ^{1}H NMR in Freon-113/$CDCL_3$: δ 1.65 (s, 6H, $2CH_3$), 2.3−2.6 (m, 12H, $2OOC(CH_2)_2-C-$ and $2CF_2CH_2$-CH_2-OOC-), 4.4 (m, 4H, $2CF_2CH_2CH_2-OOC-$).

Emulsion Polymerization. All emulsion polymerizations were conducted in a 10-mL stainless steel cylindrical high-pressure cell, equipped with two 1-cm thick sapphire windows at each end to permit visual observation. Each window was sealed with a Teflon O-ring on the high-pressure side and a brass ring on the external side secured with a stainless-steel endcap. In a typical polymerization reaction, the cell was charged with 1 g of *N*-ethylacrylamide, 0.01 g of AIBN, and the desired amount of PMAGlc-*b*-PFOMA surfactant. The reactor was first purged with a flow of CO_2 to remove air for 10 min and then filled with liquid CO_2 to approximately 145 bar by an automatic syringe pump (model No. 260D; Isco, Lincoln, NE). The cell was gradually heated to 65 °C and the pressure was increased to approximately 352 bar. The polymerization was allowed to proceed for 20 h as a small egg-shaped stir bar agitated the mixture. At the end of the reaction, the cell was cooled to room temperature and the CO_2 was slowly vented through a pressure release valve. The white polymer product was collected, and the yield was determined gravimetrically.

Initiator Thermal Decomposition Rate in CO_2. The thermal decomposition rates of both AIBN and the fluorinated azo-derivative in $scCO_2$ were recorded on a PerkinElmer Lambda 40 UV/vis Spectrometer (PerkinElmer, Norwalk, CT) at different temperatures with a constant CO_2 density of 0.85 g/mL. In a typical experiment, initiator (∼0.2 mmol) was placed in a 2.5-mL high-pressure cell equipped with two sapphire windows at each end to allow UV light to go through. The cell was first purged with CO_2 for about 20 min and then filled with CO_2 to approximately 170 bar. Gradually, the cell was heated to the desired temperature (65, 70, or 80 ± 0.1 °C). The final required pressure was achieved with the addition of more CO_2. Another 2.5-mL high-pressure cell with an identical path length was used as a reference. All UV spectra were collected once every 15 or 30 min.[28]

Characterization. ^{1}H NMR spectra were obtained in $CDCl_3$, D_2O, C_6F_6/C_6D_6, or Freon-113/$CDCL_3$ with a Bruker Avance 400 MHz spectrometer (Bruker Instruments, Bilerica, MA). Scanning Electron Microscopy (SEM) images were obtained using a JSM-6400 FE SEM (JEOL LTD, Japan). Intrinsic viscosity measurement was carried out using a Ubbelohde Viscometer (Ref. No. 52610/I, Schott-Gerate, Germany) in a water bath thermostatically controlled at 25 ± 0.1 °C by a Schott-Gerate Transparent Thermostate CT 1650 (Schott-Gerate, Germany).

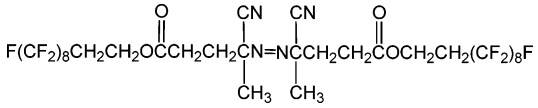

Figure 1. Structure of the fluorinated azo-derivative initiator.

Scheme 2. Emulsion Polymerization of NEAM in $ScCO_2$

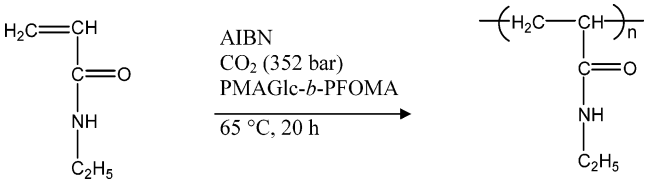

Results and Discussion

***N*-Ethylacrylamide.** CO_2 is a nonpolar molecule with a low dielectric constant and low polarizability per unit volume. Many polar or hydrophilic molecules, such as water, proteins, amides, ionic species, sugars, etc., exhibit very poor solubility in CO_2. In this report, a water-soluble acrylamide monomer, NEAM, was used for CO_2 emulsion polymerization studies. Our experiments found that NEAM had a relatively low solubility in CO_2. Under our typical CO_2 emulsion polymerization condition (65 °C, 352 bar), the solubility in CO_2 was less than 3% w/v. Phase separation occurred when monomer concentration was more than 3% w/v.

Poly(*N*-ethylacrylamide) (poly(NEAM)) is hydrophilic and water-soluble, with a glass transition temperature (T_g) around 139 °C.[29] As one of the *N*-substituted polyacrylamides, the balance between the hydrophilic amide groups and the hydrophobic substitute moieties provides poly(NEAM) with thermosensitive property. Reversible phase separation occurs when water temperature reaches 72 °C.[30] Such a high phase transition temperature makes poly(NEAM) attractive in applications such as controlled flocculation for oil recovery[31] and lignin separation in the paper industry.[32] Linear and cross-linked poly(NEAM) can be prepared by free-radical polymerization in water or in organic solvents. Aqueous emulsion polymerization of NEAM to produce cross-linked microgels has been reported.[30]

Surfactant. A hydrophilic/CO_2-philic $PMAGlc_3$-*b*-$PFOMA_{90}$ (1K-*b*-43K) block copolymer with a sugar-to-PFOMA block molar ratio of 1:30 was used as a stabilizing agent for the emulsion polymerization of NEAM in CO_2. At room temperature and a CO_2 pressure of 276 bar, this block copolymer solubility in CO_2 was measured to be more than 5% w/v. Further studies showed that, under the employed polymerization condition, the surfactant was totally miscible with CO_2. Light-scattering studies indicated that such a diblock copolymer could self-assemble into aggregates in CO_2 with an average micellar diameter of 27 nm.[21]

Emulsion Polymerization in CO_2. *Effect of the Surfactant Concentration.* Under the reaction conditions, NEAM was immiscible with CO_2 as a liquid monomer phase. The emulsion polymerization of NEAM in CO_2 in the presence of surfactant (PMAGlc-*b*-PFOMA, from 10 to 0.2 wt%, based on the monomer weight) (Scheme 2) started heterogeneously and quickly developed into a milky-white emulsion upon agitation. Once the temperature was raised to 65 °C, the solution became progressively more cloudy and finally formed a stable latex solution without phase distinction between the polymer and the CO_2 throughout the whole reaction (20 h). The only exception is the reaction with 0.2 wt% surfactant concentration, in which the produced polymer eventually separated from the CO_2 continuous phase. After cooling and depressurization, the resulting polymer was easily isolated as a white powder in high yield (>90%).

We also performed two other comparison experiments: one with 10 wt% of PMAIpGlc-*b*-PFOMA (1:30), the hydrophobic/CO_2-philic surfactant with the protected sugar block before hydrolysis, and another without any surfactant. In both cases, initially the liquid monomer was easily dispersed within the continuous CO_2 phase but remained as clear liquid droplets which would settle very quickly after the agitation was stopped. No cloudy, kinetically stable white emulsion was observed. During the polymerization of these systems, precipitates occurred quickly after the temperature reached 65 °C. After CO_2 depressurization, the resulting polymer was found to accumulate as a thick film on the interior walls and as a solid mass at the bottom of the cell with yields of 90% (with 10 wt% of PMAIpGlc-*b*-PFOMA) and 88% (without surfactant), respectively. It appears that the hydrophilic form of the surfactants, PMAGlc-*b*-PFOMA, was necessary to enable effective emulsification of the system to stabilize the water-soluble and CO_2-insoluble poly(NEAM) in CO_2. The hydrogen-bonding interactions between the PMAGlc-*b*-PFOMA pendent sugar rings and NEAM and its resulting polymer were necessary to realize effective interactions. Similar hydrogen-bonding interactions have been observed by Howdle, et al.[10] in dispersion polymerization of methyl methacrylate in CO_2 using a carboxylic acid-terminated perfluoropolyether stabilizer. The data for all of the polymerization reactions are summarized in Table 1. ^{1}H NMR did not detect monomer in any of the polymer products.

SEM was used to examine the morphology of the isolated products. Discrete spherical particles in submicrometer sizes were observed (Figure 2a−e) for all reactions which used PMAGlc-*b*-PFOMA at concentrations of 10, 5, 2, 0.5, and 0.2 wt%. Some coagulated particles were also observed in the reaction with the lowest concentration of the PMAGlc-*b*-PFOMA surfactant used (0.2 wt%). Clearly, as the surfactant concentration decreased, the particle diameter increased from the submicrometer range to ~1 μm. In an emulsion polymerization, the number of polymer particles formed is associated with the surfactant concentration. With more surfactant molecules, the number of surfactant-stabilized micelles increases, resulting in smaller-sized particles.[29] In the polymerizations with the protected block copolymer PMAIpGlc-*b*-PFOMA (Figure 3a) and without surfactant (Figure 3b), irregular polymer products with highly agglomerated morphology predominated.

At low surfactant concentrations (0.5 and 0.2 wt%), surprisingly, some large particles with a size much larger than 1 μm in diameter were seen in addition to the submicrometer-sized particles that are typical for most emulsion polymerization and for that found herein at higher surfactant concentrations (Figure 4a and b). We believe that these large particles were produced from the polymerized monomer droplets (bulk polymerization, as in suspension) since the AIBN initiator is soluble in both CO_2 and the liquid monomer phase. Initiation took place not only in the polymerization medium but also inside the monomer droplets. Kast et

Table 1. Data for the Polymerizations of NEAM in CO_2[a]

[*S*], wt%[b]	initial state	final state	yield, %[c]	*Dn*[d]	PSD[e]
10	emulsion	latex	90	spherical 0.15 μm	1.41
5	emulsion	latex	95	spherical 0.25 μm	1.52
2	emulsion	latex	90	spherical 0.48 μm	1.53
0.5	emulsion	latex	90	spherical <1 μm, >1 μm	bimodal
0.2	emulsion	ppt	88	some coagulated <1 μm, >1 μm	bimodal
10 wt% protected	NEAM droplets	ppt	90	irregular	
no surfactant	NEAM droplets	ppt	88	irregular	

[a] Reaction conditions: 10 mL CO_2 cell; 1 g NEAM; 0.01 g AIBN; 65 °C; 352 bar; 20 h. [b] Based on the monomer weight. [c] Yields were determined gravimetrically. [d] Mean particle diameter measured from SEM analysis. [e] Particle size distribution, *Dw*/*Dn*, from SEM analysis.

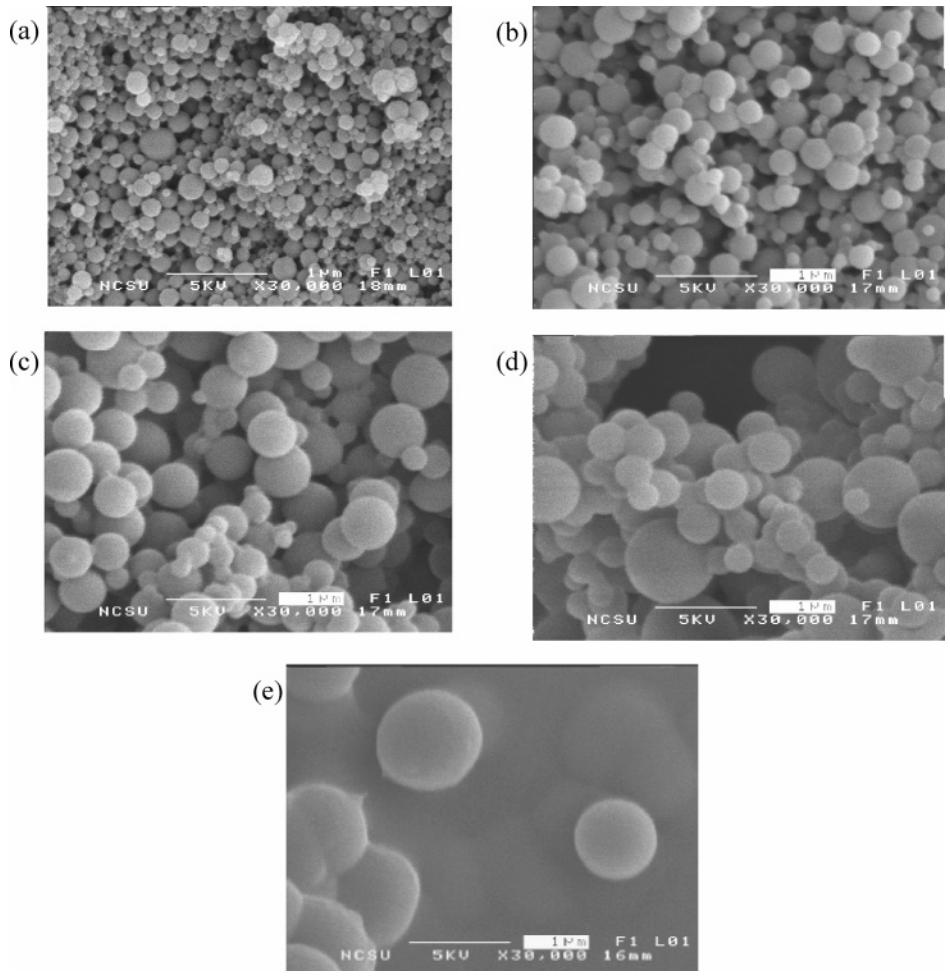

Figure 2. SEM images of poly(NEAM) particles produced at various PMAGlc-*b*-PFOMA surfactant concentrations: (a) 10, (b) 5, (c) 2, (d) 0.5, and (e) 0.2 wt%. Reaction conditions: 1 g NEAM; 0.01 g AIBN; 65 °C; 352 bar; 20 h.

al.,[34] who studied a bimodal polymerization involving both emulsion and suspension, have reported that large particles (0.5−10 μm) were found in that system and that the amount of polymerized monomer droplets depended strongly on the surfactant concentration. At a high surfactant concentration, monomer could be completely emulsified prior to polymerization. Therefore, the polymerization began in monomer-containing micelles (emulsion), resulting in submicrometer-size particles instead of large particles from the polymerized monomer droplets. Here, we have not observed such large particles in the three other reactions with higher surfactant concentrations (10, 5, and 2 wt%). The high yields of irregular polymer from the reactions with 10 wt% protected PMAIpGlc-*b*-PFOMA and without surfactant were also contributed to the complete polymerizations in monomer droplets. Later, we will discuss the NEAM emulsion polymerization initiated by a CO_2-soluble but monomer-insoluble initiator, a fluorinated AIBN; as expected, only polymerized micelle particles were obtained.

Effect of the Initiator (AIBN) Concentration. The CO_2 emulsion polymerization of NEAM has been carried out at three different AIBN initiator concentrations: 0.5,

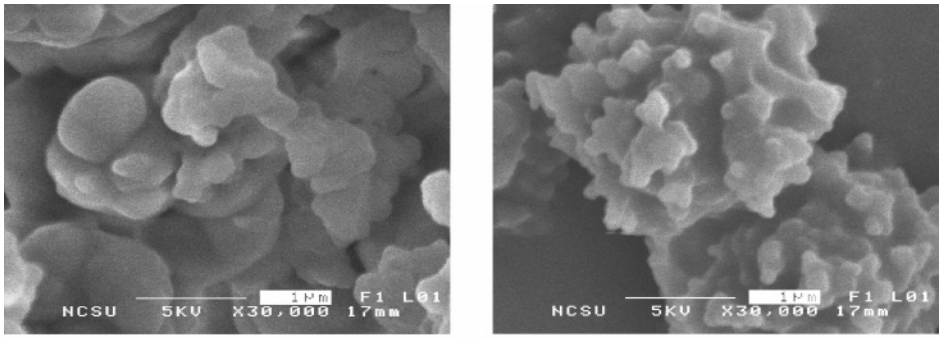

Figure 3. SEM images of poly (NEAM) particles produced using (a) 10 wt% of poly(MAIpGlc-*b*-PFOMA) and (b) 0 wt% surfactant. Reaction conditions: 1 g NEAM; 0.01 g AIBN; 65 °C; 352 bar; 20 h.

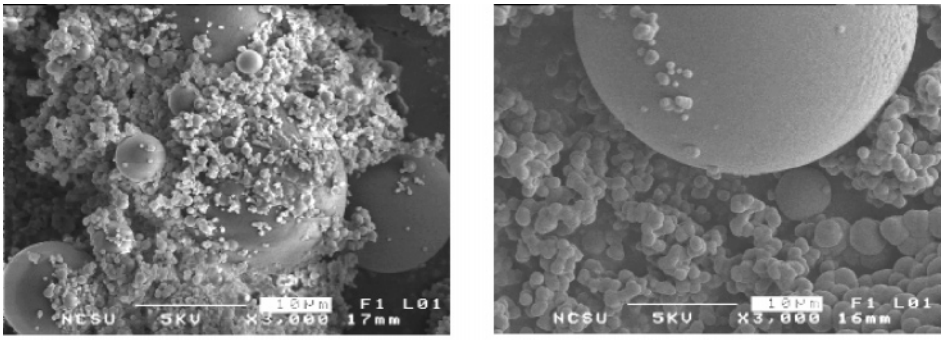

Figure 4. SEM of large particles coexisting with submicrometer particles from the reaction with (a) 0.5 and (b) 0.2 wt% PMAGlc-*b*-PFOMA surfactant. Reaction conditions: 1 g NEAM; 0.01 g AIBN; 65 °C; 352 bar; 20 h.

Table 2. Polymerizations with Different Initiator (AIBN) Concentrations[a]

[*I*] wt%[b]	initial state	final state	yield %[c]	particle morphology, D_n[d]
0.5	emulsion	latex	94	spherical, 0.34 μm
1.0	emulsion	latex	95	spherical, 0.25 μm
2.0	emulsion	latex	95	spherical, 0.11 μm

[a] Reaction conditions: 1 g NEAM; 0.05 g PMAGlc-*b*-PFOMA; 65 °C; 352 bar; 20 h. [b] Based on the monomer weight. [c] Yields were determined gravimetrically. [d] Mean particle diameter from SEM analysis.

1.0, and 2.0 wt% (based on the monomer weight). In all three cases, the contents of PMAGlc-*b*-PFOMA and NEAM were kept constant at 0.05 and 1.0 g, respectively. An initial monomer-emulsified solution and a final white latex were observed in all three reactions and the resulting white polymer powders were collected with isolated yields of approximately 95% (Table 2). Figure 5 displays the SEM images of poly(NEAM) obtained from these reactions. As the initiator concentration increased, particle size decreased. Many authors have reported similar results,[5,35−39] which is in accordance with the nucleation mechanism of an emulsion polymerization. In an emulsion polymerization, the nucleation of particles takes place in either the monomer-swollen micelles[40] (which are further transformed into polymer particles by absorption of radicals from the medium phase) or the precipitated solution-polymerized oligomer radicals (homogeneous nucleation).[41,42] The formation of polymer particles through both micellar and homogeneous nucleation involves the absorption of surfactant from the micelles, medium, and monomer droplets, and the number of polymer particles, N, is dependent on the total surfactant surface area present in the system and the initiation rate. The same result (eq 1) has been derived for both micellar and homogeneous nucleation[33,40,43]

$$N = \kappa(R_i/\mu)^{0.4}S^{0.6} = KI^{0.4}S^{0.6} \quad (1)$$

where κ and K are constants, μ is the rate of volume increase of a polymer particle, R_i and I the initiation rate and the initiator concentration, and S the surfactant concentration. Obviously, with more initiator and surfactant, the emulsion polymerization leads to more polymer particles, which are associated with a smaller particle size.

Effect of the Reaction Temperature. As it is well known, the number of polymer particles, N, plays a dominant role in the determination of the rate and degree of emulsion polymerization where N depends on the initiation rate. Having seen the effect of initiator concentration on the particle size, we performed two comparison experiments at different reaction temperatures (65 and 80 °C). Since the solvency of CO_2 depends mainly on the CO_2 density, which can be easily manipulated by changing the system temperature and pressure, here we kept the same CO_2 density (0.85 g/mL) in order to maintain the same CO_2 solvency. The PMAGlc-*b*-PFOMA surfactant and AIBN initiator were 5 and 1 wt% based on the monomer weight. At 65 and 80 °C, the corresponding pressures were 352 and 430 bar, respectively. A stable latex colloidal solution was observed during the reaction time, and both polymerizations were completed with ∼100% monomer conversions. Not surprisingly, much smaller particles were observed in the reaction at the higher reaction temperature (Figure 6). Higher temperatures usually result in a fast initiation rate. In a later section (see Table 5) we

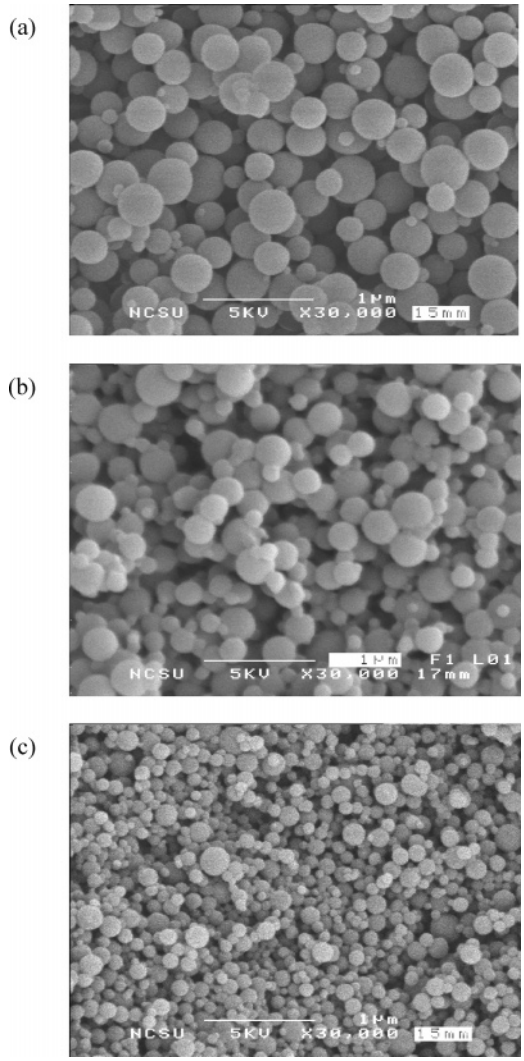

Figure 5. SEMs of poly(NEAM) latex particles obtained from three reactions conducted with (a) 0.5, (b) 1.0, and (c) 2.0 wt% AIBN (based on the weight of NEAM). Reaction conditions: 1 g NEAM; 0.05 g PMAGlc-*b*-PFOM; 65 °C; 352 bar; 20 h.

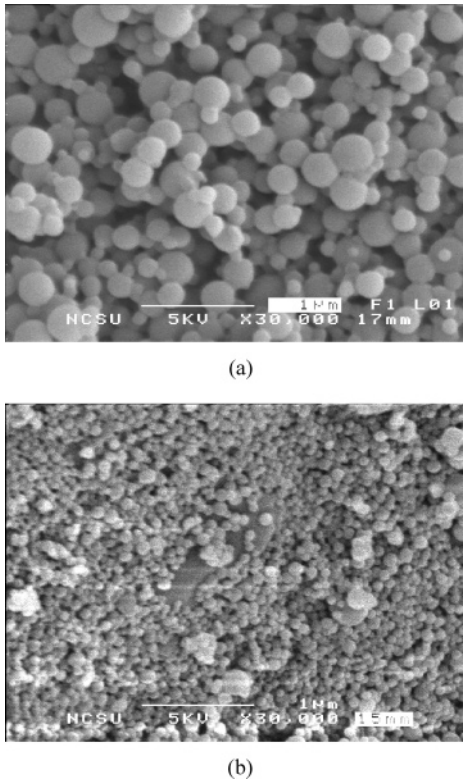

Figure 6. Poly(NEAM) particles from the reactions at 65 (a) and 80 °C (b). Reaction conditions: 1 g NEAM; 0.01 g AIBN; 0.05 g PMAGlc-*b*-PFOM; 20 h; $d_{CO_2} = 0.85$ g/mL.

Table 3. NEAM Emulsion Polymerizations at Different Monomer Concentrations[a]

[*M*] % w/v	initial state	final state	yield[b] %	particle morphology
10	emulsion	latex	95	spherical, 0.25 μm
20	emulsion	latex	92	spherical, 0.16 μm
30[c]	emulsion	ppt	99	spherical, 0.21 μm

[a] Reaction conditions: 5 wt% PMAGlc-*b*-PFOMA; 1 wt% AIBN; 65 °C; 352 bar; 20 h. (wt% is based on the total added monomer weight.) [b] Yields were determined gravimetrically. [c] A short-time autoacceleration reaction took place, $T \rightarrow 90$ °C.

studied the thermal decomposition of AIBN in $scCO_2$, and the rate constants of AIBN in CO_2 at 80 and 65 °C were 7.34×10^{-5} S^{-1} and 0.97×10^{-5} S^{-1}, respectively. According to eq 1, in an emulsion polymerization with a high initiation rate, R_i, a large number of polymer particles are expected to form during the nucleation and relatively smaller-sized polymer beads could be obtained.[38,39]

Effect of the Monomer Concentration. Emulsion polymerizations at three different monomer concentrations (10, 20, and 30% w/v) were conducted in 352 bar CO_2 at 65 °C (Table 3). In all cases, the weight ratios of AIBN and PMAGlc-*b*-PFOMA to NEAM monomer were fixed at 1 and 5 wt%, respectively. When the temperature reached 65 °C, dispersed stable colloids were observed for all three reactions. However, for the reaction with the highest monomer concentration (30% w/v), the temperature abruptly rose to 90 °C for a few minutes and then came down to 65 °C, after which flocculation occurred immediately. Since the ratio of monomer/surfactant/initiator was kept constant, theoretically[33,40,43] there should be no change in particle diameter. However, the size change was observed in our system. Figure 7 shows the scanning electron micrographs of poly(NEAM) particles obtained from these three reactions. Discrete spherical particles were imaged, even including the reaction with 30% w/v monomer concentration in which the resulting product was agglomerated. Compared with the reaction at 10% w/v solids, the particles produced at 20% w/v solids had an obviously smaller size. When the monomer input increased to 30% w/v, the particles became larger again. Although no direct evidence exists, the change of particle sizes may be caused by the differential rate of polymerization. With increased monomer concentration and accordingly more initiator and surfactant, the polymerization rate was tremendously enhanced. In the reaction with 30% w/v NEAM, we have seen a vigorous gel effect (abrupt temperature rise) and aggregation at the primary stage of polymerization, which is probably due to the fast nucleation and a relatively high viscosity within the polymer particles.

Effect of the CO_2 Pressure. An opportunity unique to supercritical fluids as a reaction medium is the ability to adjust its solvent quality through its easily tunable density and dielectric constant by simply changing either pressure or temperature. Moreover, for free-radical reactions, CO_2 offers no chain transfer to solvent

Table 4. NEAM Emulsion Polymerizations at Different Pressures[a]

pressure, bar	CO_2 density[c]	initial state	final state	yield[b], %	particle morphology	D_n[d], μm	PSD[e]
276	0.79	emulsion	latex	100	spherical	0.19	1.07
352	0.85	emulsion	latex	95	spherical	0.25	1.52
428	0.89	emulsion	ppt	94	spherical	small: 0.11 big: 0.72	bimodal

[a] Reaction conditions: 1 g NEAM; 0.05 g PMAGlc-*b*-PFOMA; 0.01 g AIBN; 65 °C; 20 h. [b] Yields were determined gravimetrically. [c] CO_2 density: g/mL. [d] Mean particle diameter, from SEM analysis. [e] Particle size distribution, from SEM analysis.

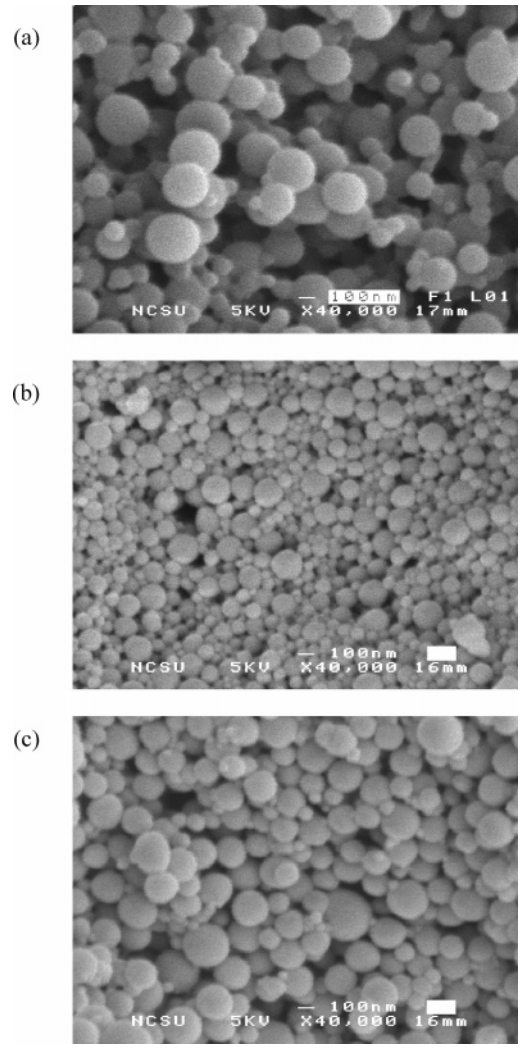

Figure 7. Scanning electron micrographs of poly(NEAM) particles obtained from the reactions with (a) 10, (b) 20, and (c) 30% w/v NEAM. Polymerization conditions: at 352 bar and 65 °C for 20 h, with 5 wt% PMAGlc-*b*-PFOMA and 1 wt% AIBN based on the added monomer weight. For the experiment with 30 wt% NEAM (c), the polymerization exotherm overroad the temperature control system and the reaction temperature of the system briefly rose to 90 °C.

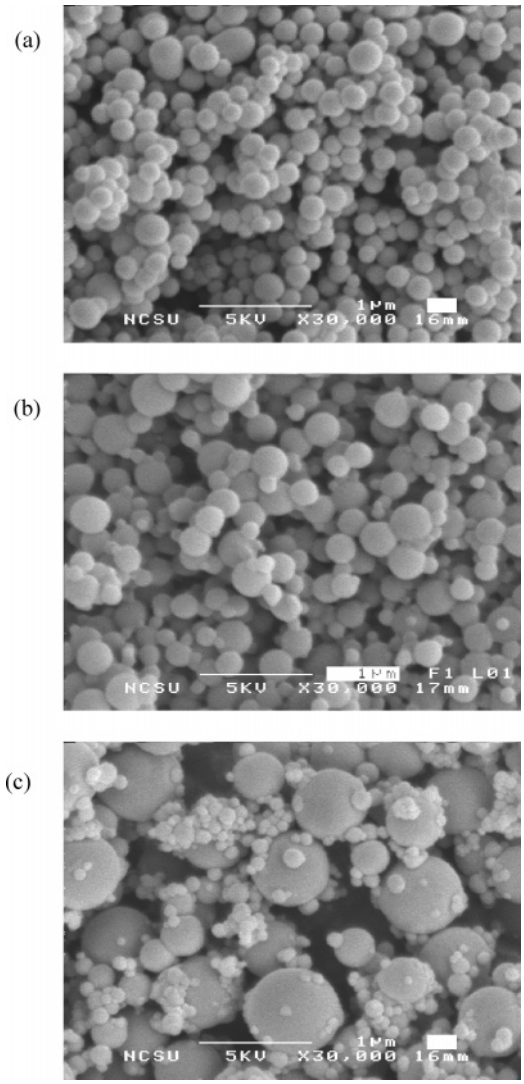

Figure 8. Poly(NEAM) particles from the reactions at the CO_2 pressures of (a) 276 bar (4000 psi), (b) 352 bar (5100 psi), and (c) 428 bar (6200 psi). Reaction conditions: 1 g NEAM; 0.05 g PMAGlc-*b*-PFOMA; 0.01 g AIBN; 65 °C; 20 h.

and high free-radical initiation efficiency with acceptable initiator decomposition kinetics.[44] The emulsion polymerization of NEAM in $scCO_2$ was conducted at three different pressures (Table 4). All reactions were performed with the same amount of monomer (10% w/v), initiator (AIBN, 1 wt% based on the monomer weight), and surfactant (PMAGlc-*b*-PFOMA, 5 wt% based on the monomer weight) at 65 °C for 20 h. Stable polymer colloids were observed for the reactions at 276 and 352 bar, but precipitation subsequently took place at a higher pressure of 428 bar. During the reactions, the corresponding CO_2 densities were 0.79, 0.85, and 0.89 g/mL. All three reactions achieved high yields (≥94%), and free-flowing powders were isolated.

When the initial pressure was increased from 276 to 352 bar, slightly larger and less uniform particles were obtained (Figure 8a and b). The reaction at the highest pressure of 428 bar displayed a bimodal size distribution (Figure 8c) with many small (0.11 μm) and large particles (0.72 μm). As the pressure increased, the CO_2 solvency of the monomer and growing polymer chains increased. The higher CO_2 solvency could affect the fraction of the monomer molecularly dissolved in the polymerization medium, which plays a key role in determining the size of the final polymer particles.[5] In addition, increased pressure could also affect the initiation rate. We[28] have previously investigated the AIBN

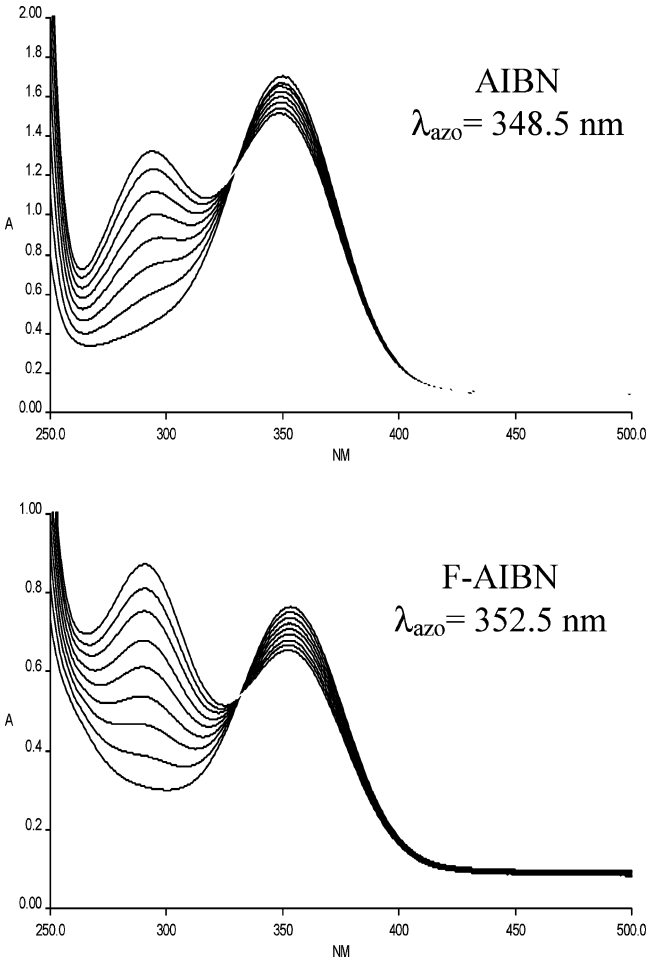

Figure 9. UV spectra for the thermal decomposition of AIBN and the fluorinated initiator in $scCO_2$ at 65 ° C and 352 bar (the spectra were collected once every 30 min).

Table 5. Rate Constant, K_d, of Thermal Decomposition of AIBN and the Fluorinated Azo-Derivative Initiator in Supercritical CO_2 at Various Temperatures[a]

T, °C	$K_{d,AIBN}$, S^{-1}	$K_{d,F-AIBN}$, S^{-1}
65	0.97×10^{-5}	1.24×10^{-5}
70	1.93×10^{-5}	2.20×10^{-5}
80	7.34×10^{-5}	7.84×10^{-5}

[a] CO_2 density: 0.85 g/mL.

thermal decomposition in $scCO_2$ as a function of pressure and found that there were two opposite effects on the decomposition rate of AIBN in $scCO_2$: the solvation effect and the intrinsic activation volume effect. In the low-pressure region, the AIBN decomposition rate was enhanced with pressure due to the solvation effect. However, as the pressure increased, the intrinsic activation volume effect dominated, which tended to lower the rate of decomposition. A maximum rate constant was observed when the pressure increased continuously. Here we see how the pressure change affected the NEAM emulsion polymerization in CO_2 is a very complicated process, and further experiments are needed to clarify the details.

Emulsion Polymerization of NEAM in CO_2 Using the Fluorinated Azo-Derivative as an Initiator. As discussed before, polymerized monomer droplets could be observed in the emulsion polymerization with a monomer-soluble initiator. To compare with the AIBN-initiated CO_2 emulsion polymerization of NEAM, a highly CO_2-philic initiator, the fluorinated AIBN derivative, was synthesized. This highly fluorinated initiator is insoluble in many organic solvents, such as CCl_4, $CHCl_3$, toluene, benzene, DMF, acetonitrile, water, etc., but is highly soluble in Freon-113 and CO_2 (>10% w/v). Most importantly, this fluorinated initiator was determined to be insoluble in the NEAM liquid monomer at temperatures ranging from room temperature to 80 °C.

Initiator Thermal Decomposition in $scCO_2$. To compare the AIBN and the fluorinated azo-derivative initiator thermal decomposition rates at the employed emulsion polymerization conditions, before performing the polymerization, we investigated both initiator thermal decompositions in $scCO_2$ using UV/visible spectroscopy. The thermal decomposition rates were recorded at different temperatures (65, 70, or 80 °C). To maintain the same CO_2 solvency as we changed the temperature, we kept the CO_2 density constant at 0.85 g/mL. The corresponding pressures at temperatures of 65, 70, and 80 °C were 352 bar (~5100 psi), 375 bar (~5400 psi), and 430 bar (~6100 psi). Figure 9 gives two typical series of UV/vis spectra of AIBN and the fluorinated initiator collected once every 30 min in $scCO_2$ at 65 °C and 352 bar. Obviously, the thermal decomposition behavior of the fluorinated AIBN derivative is analogous to that of AIBN. The decreased azo absorptions at 348.5 nm for AIBN and 352.5 nm for the fluorinated azo initiator corresponded to the loss of azo groups during thermal decomposition, and the increased absorptions at 292.5 nm corresponded to a temporary product, ketenimine ($Me_2(CN)-C-N=C=C-Me_2$).[28,45] The rates of AIBN and the fluorinated initiator thermal decomposition were also measured at 70 and 80 °C at the same CO_2 density as that at 65 °C and 352 bar (i.e., d = 0.85 g/mL). According to the first-order kinetics of the initiation reaction,[29] the calculated AIBN and the fluorinated azo-derivative initiator rate constants (K_d) are shown in Table 5. Obviously, the initiation rate constant increased with temperature. For each temperature, the K_d of the fluorinated azo initiator is slightly higher than that of AIBN. On the basis of the Arrhenius plot,[33] the activation energies of the decomposition of AIBN and the fluorinated initiator in $scCO_2$ were

Table 6. NEAM Emulsion Polymerizations with the Fluorinated Initiator[a]

[S], wt%[b]	initial state	final state	yield, %[c]	particle morphology, D_n[d]	PSD[e]
10	emulsion	latex	100	spherical 0.14 μm	1.11
5	emulsion	latex	90	spherical 0.27 μm	1.16
2	emulsion	latex	93	spherical 0.50 μm	1.16
0.5	emulsion	ppt	88	spherical 0.91	1.18
0.2	emulsion	ppt	94	spherical 1.48 μm	1.29
protected	NEAM droplets	ppt	40	irregular	
no surfactant	NEAM droplets	ppt	25	irregular	

[a] Reaction conditions: 1 g NEAM; 0.061 mmol F-AIBN; varied amount of PMAGlc-*b*- PFOMA (1:30); 65 °C; 352 bar; 20 h. [b] Based on the monomer weight. [c] Yields were determined gravimetrically. [d] Mean particle diameter from SEM analysis. [e] Particle size distribution, *Dw*/*Dn*, from SEM analysis.

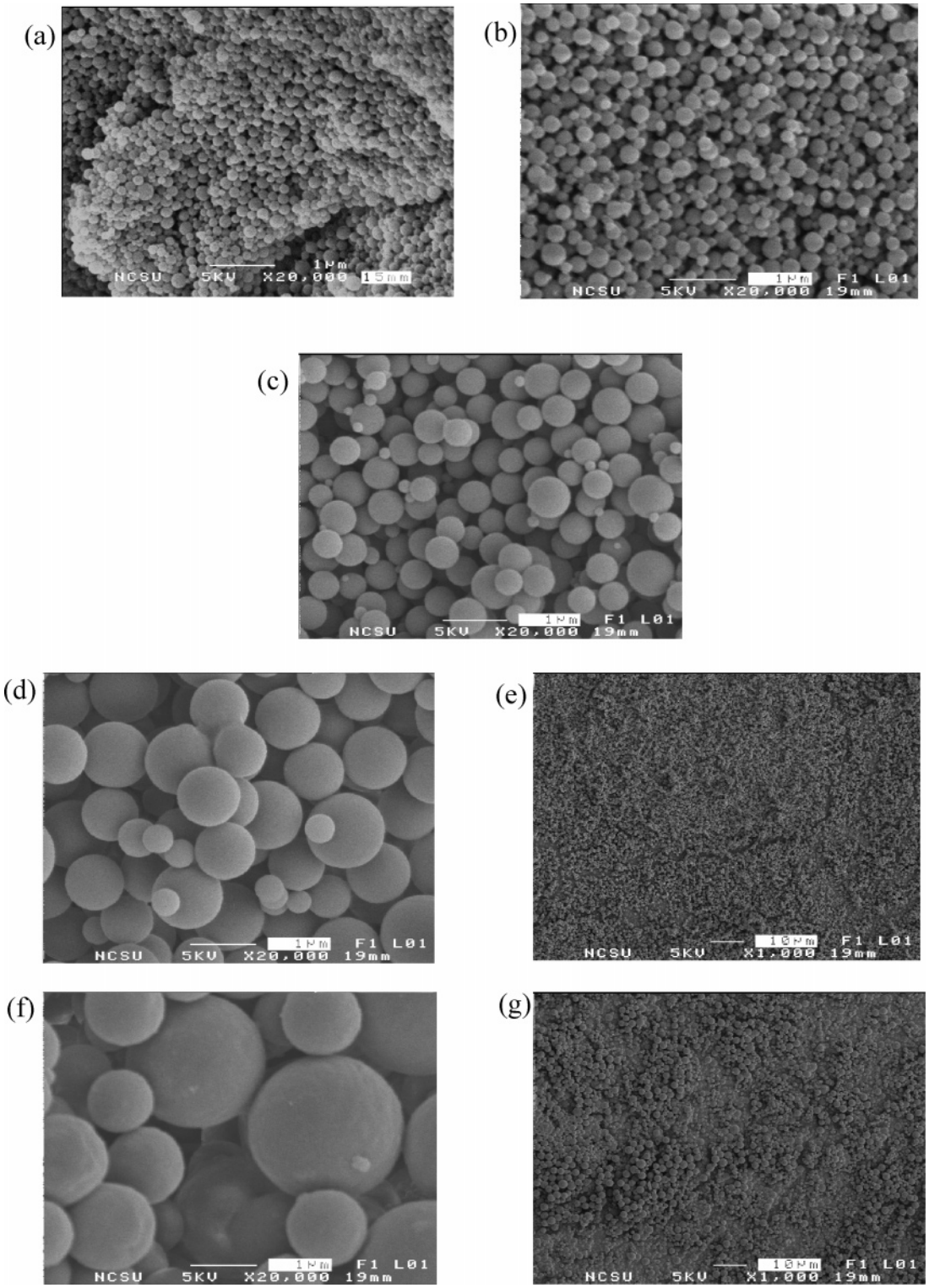

Figure 10. SEM images of poly(NEAM) particles prepared from the fluorinated azo-derivative-initiated CO_2 emulsion polymerization with different PMAGlc-*b*-PFOM concentrations. (a) 10, (b) 5, (c) 2, (d) and (e) 0.5, (f) and (g) 0.2 wt%. Reaction conditions: 1 g NEAM; 0.061 mmol of the fluorinated initiator; 65 °C; 352 bar; 20 h.

calculated to be 133.8 and 122.7 kJ/mol, respectively. The activation energy of AIBN is in good agreement with the published values of 134.6[28] and 128.3 kJ/mol[45] measured in $scCO_2$. By comparing the two different initiation systems in which the fluorinated azo-derivative is only preferentially soluble in the CO_2 phase while AIBN partitions itself between the CO_2 and monomer phases, we further investigated the fluorinated initiator-initiated emulsion polymerization of NEAM in $scCO_2$.

Emulsion Polymerization of NEAM Initiated by the Fluorinated Initiator. Table 6 gives the summary of the performed reactions initiated by the fluorinated azo-derivative initiator. All reaction conditions (65 °C, 352 bar, 20 h) were kept the same as in the AIBN-initiated system, in which the same concentration of initiator, 0.061 mmol, was added. Spherical particles (Figure 10) with high yields (~90%) were produced, and the particle size decreased with the amount of surfactant (from 10

Table 7. Intrinsic Viscosity Data of Poly(NEAM) Products[a]

surfactant concentration wt%[b]	EtSH mmol	AIBN [η] 100 mL/g	F-AIBN [η] 100 mL/g
0.2		1.38	1.64
0.5		1.61	1.63
5.0		2.57	2.07
5.0	0.27	0.16	
5.0	1.35	0.10	

[a] Reaction conditions: 1 g NEAM; 0.061 mmol initiator; 65 °C; 352 bar; 20 h. [b] Based on the monomer weight.

to 0.2 wt%). No significant size difference in the particles initiated by AIBN and the fluorinated initiator was observed. However, apparently the particles from the fluorinated initiator system were more uniform with relatively narrowed particle size distribution, and no polymerized monomer droplets were observed even at the very low surfactant concentrations (Figure 10d−g). As discussed before, unlike AIBN, the fluorinated azo initiator was found to be insoluble in the monomer phase and therefore is preferentially located in the CO_2 phase. As such, there is essentially no initiator partitioning into the monomer droplets. Instead of the polymerization process in the AIBN-initiated system involved in more than one set of defined polymerization mechanisms, the fluorinated initiator initiated emulsion polymerization of NEAM in $scCO_2$ follows a typical emulsion polymerization in which polymerization essentially occurs in active micelles, the polymer particles. As anticipated, uniform particles, without large particles from the polymerized monomer droplets, were observed. In addition, two comparison experiments were performed, both initiated by the fluorinated initiator: one with 10 wt% of the protected PMAIpGlc-*b*-PFOMA and the other without any surfactant. Sticky and gel-like irregular products were recovered, and the yields were as low as 40% (with 10 wt% PMAIpGlc-*b*-PFOMA) and 25% (without surfactant), respectively. In contrast, the corresponding AIBN-initiated reactions resulted in the formation of dry polymer aggregates with high yields around 90%. Further intrinsic viscosity measurements found that these dry polymer aggregates had a relatively higher molecular weight than that of the gel-like products initiated by the fluorinated initiator. It is suspected that the high yields and high molecular weight in the AIBN-initiated polymerization system are a result of the ability of AIBN to partition into the NEAM monomer droplets followed by the complete polymerization of the monomer droplets.

Under controlled reaction time in the presence of 5 wt% PMAGlc-*b*-PFOMA, we found that the NEAM emulsion polymerization in $scCO_2$ initiated by either AIBN or the fluorinated azo-derivative initiator was very fast—the first 5 min of the reaction resulted in a gel-like product with an isolated yield of 50% for the fluorinated initiator system and 70% for the AIBN-initiated reaction. Dry polymer in the form of a powder was obtained after 20 min, and monomer conversions were found to be more than 90%. After 20 min, the reaction was almost complete, with separate particles fully formed and stabilized without further size and distribution changes.

Table 7 gives the results of viscosity measurements on the poly(NEAM) produced from the reactions with different surfactant concentrations. The intrinsic viscosity, [η], was conducted by extrapolation to infinite dilution, according to the Huggins equation.[46] In both AIBN and the fluorinated azo-derivative-initiated polymerizations, the molecular weight, represented by the intrinsic viscosity, increased with the amount of employed surfactant, which is in good agreement with the theoretical prediction that the number of created particles depends on the surfactant concentration (eq 1), and the molecular weight is proportional to the number of particles.[33] As for the polymers produced from the different initiators, no direct conclusion on the molecular weight could be drawn (Table 7). On one hand, the rate constant of the fluorinated initiator decomposition in $scCO_2$ is only slightly higher than the value of AIBN; on the other hand, in the AIBN-initiated reactions, the initiation could take place inside the liquid monomer droplets, which makes the polymerization mechanism complicated. However, the measured intrinsic viscosities in both systems are much larger than a typical value from the NEAM solution polymerization ([η] = 0.20). It is well known that emulsion polymerization can generally produce polymers with high molecular weight ($\sim 10^6$).[19] Having tested the reactions with ethyl mecaptan (EtSH) as a chain transfer agent in $scCO_2$, we found that the intrinsic viscosities dropped tremendously (depends on the amount of EtSH, see Table 7) and, thus, the poly(NEAM) molecular weight could be controlled.

Conclusions

An emulsion polymerization to prepare water-soluble polymers from supercritical CO_2 phase has been investigated herein. With the aid of a sugar-containing CO_2 amphiphile, the hydrophilic poly(NEAM) could be stabilized as a stable colloid in CO_2 continuous phase and recovered as spherical particles in the range of submicrometer size. It was found that the concentration of monomer, emulsifier, and initiator and the CO_2 pressure and temperature had substantial effects on the size of the colloidal particles. Two CO_2-soluble initiators, AIBN and a highly CO_2-philic, monomer-insoluble, fluorinated azo-derivative were used. Some large particles from the polymerized monomer droplets (>1 μm) were only observed in the AIBN-initiated system. Viscosity measurements indicated that the molecular weight of poly(NEAM) increased with the amount of surfactant and could be adjusted by chain transfer agents.

Acknowledgment. This material is based upon work supported by the STC Program of the National Science Foundation under Agreement No. CHE-9876674.

References and Notes

(1) Canelas, D. A.; DeSimone, J. M. *Adv. Polym. Sci.* **1997**, *133*, 103.
(2) Kendall, J. L.; Canelas, D. A.; Young, J. L.; DeSimone, J. M. *Chem. Rev*. **1999**, *99*, 543.
(3) Cooper, A. I. *J. Mater. Chem*. **2000**, *10*, 207.
(4) DeSimone, J. M.; Guan, Z.; Elsbernd, C. S. *Science* **1992**, *257*, 945.
(5) Arshady, R. *Colloid Polym. Sci.* **1992**, *270*, 717.
(6) DeSimone, J. M.; Maury, E. E.; Menceloglu, Y. Z.; McClain, J. M.; Romack, T. J.; Combes, J. R. *Science* **1994**, *265*, 356.
(7) Betts, D. E. The Synthesis, Characterization, and Application of CO_2-Soluble, Non-Ionic Amphiphilic Block Copolymers. Ph.D. Dissertation, University of North Carolina at Chapel Hill, 1998.
(8) Hsiao, Y.-L.; Maury, E. E.; DeSimone, J. D.; Mawson, S.; Johnston, K. P. *Macromolecules* **1995**, *28*, 8159.
(9) Canelas, D. A.; DeSimone, J. M. *Macromolecules* **1997**, *30*, 5673.
(10) Christian, P.; Howdle, S. M. *Macromolecules* **2000**, *33*, 237.

(11) Shiho, H.; DeSimone, J. M. *Macromolecules* **2000**, *33*, 1565.
(12) Shiho, H.; DeSimone, J. M. *Macromolecules* **2001**, *34*, 1198.
(13) Shiho, H.; DeSimone, J. M. *J. Polym. Sci., Part A: Polym. Chem.* **2000**, *38*, 1146.
(14) Shiho, H.; DeSimone, J. M. *J. Polym. Sci., Part A: Polym. Chem.* **2000**, *38*, 3783.
(15) Romack, T. J.; Maury, E. E.; DeSimone, J. M. *Macromolecules* **1995**, *28*, 912.
(16) Romack, T. J.; DeSimone, J. M.; Treat, T. A. *Macromolecules* **1995**, *28*, 8429.
(17) Cooper, A. I.; Hems, W. P.; Holmes, A. B. *Macromol. Rapid Commun*. **1998**, *19*, 353.
(18) Quadir, M. A.; Snook, R.; Gilbert, R. G.; DeSimone, J. M. *Macromolecules* **1997**, *30*, 6015.
(19) Adamsky, F. A.; Beckman, E. J. *Macromolecules* **1994**, *27*, 312.
(20) Hile, D. D.; Pishko, M. V. *J. Polym. Sci.,. Part A: Polym. Chem.* **2001**, *39*, 562.
(21) Ye, W.; Wells, S.; DeSimone, J. M. *J. Polym. Sci.,. Part A: Polym. Chem.* **2001**, *39*, 3841.
(22) Bergmann, F.; Weixmann, M.; Dimant, E.; Patai, J.; Samuskowica, J. *J. Am. Chem. Soc*. **1948**, *70*, 1612.
(23) Harmon, R. E.; Jensen, B. L.; Gupta, S. K.; Nelson, J. D. *J. Org. Chem*. **1970**, *35*, 825.
(24) Shea, K. J.; Stoddard, G. J.; Shavelle, D. M.; Wakui, F.; Choate, R. M. *Macromolecules* **1990**, *23*, 4497.
(25) Liu, H. Y.; Zhu, X. X. *Polymer* **1999**, *40*, 6985.
(26) Smith, D. *Makromol. Chem.* **1967**, *103*, 301.
(27) DeSimone, J. M.; Maury, E. E.; Combes, J. R.; Menceloglu, Y. Z. *Polym. Mater. Sci. Eng.* **1993**, *68*, 41.
(28) Guan, Z.; Combes, J. R.; Menceloglu, Y. Z.; DeSimone, J. M. *Macromolecules* **1993**, *26*, 2663.
(29) Nichifor, M.; Zhu, X. X. *Polymer* **2003**, *44*, 3053.
(30) Lowe, J. S.; Chowdhry, B. Z.; Parsonage, J.; Snowden, M. J. *Polymer* **1998**, *39*, 1207.
(31) Xue, W.; Huglin, M. B.; Jones, T. G. J. *Macromol. Chem. Phys*. **2003**, *204*, 1956.
(32) Cai, W.; Gupta, R. B. *Ind. Eng. Chem. Res*. **2001**, *40*, 3406.
(33) Odian, G. *Principles of Polymerization*; John Wiley and Sons: New York, 1991.
(34) Kast, H.; Funke, W. *Makromol. Chem*. **1981**, *182*, 1567.
(35) Herrera-Ordonez, J.; Olayo, R. *J. Polym. Sci., Part A: Polym. Chem.* **2001**, *19*, 2547.
(36) Vidotto, G.; Arrialdi, A. C.; Talamini, G. *Makromol. Chem*. **1970**, *134*, 41.
(37) Gardon, J. L. *J. Polym. Sci. A* **1968**, *6*, 643.
(38) Nomura, M.; Kodani, T.; Ojima, J.; Kihara, Y.; Fujita, K. *J. Polym. Sci., Part A: Polym. Chem.* **1998**, *36*, 1919.
(39) Xu, Z.; Yi, C.; Cheng, S.; Feng, L. *J. Appl. Polym*. **2001**, *79*, 528.
(40) Smith, W. V.; Ewart, R. W. *J. Chem. Phys.* **1948**, *16*, 592.
(41) Hansen, F. K.; Ugelstad, J. *J. Polym. Sci., Part A: Polym. Chem.* **1978**, *16*, 1953.
(42) Fitch, R. M.; Prenosil, M. B.; Sprick, K. J. *J. Polym. Sci*. **1969**, *C27*, 95.
(43) Roe, C. P. *Ind. Eng. Chem.* **1968**, *16*, 592.
(44) Bunyard, C. W.; Kadla, J. F.; DeSimone, J. M. *J. Am. Chem. Soc*. **2001**, *123*, 7199.
(45) Morris, R. E.; Mera, A. E.; Brady, R. F. *Fuel* **2000**, *79*, 1101.
(46) Huggins, M. L. *J. Am. Chem. Soc*. **1942**, *64*, 2716.

MA048863Q